

# Study of QCD Phase Diagram with Non-Zero Chiral Chemical Potential

V. V. Braguta,<sup>1,2,3,4</sup> E.-M. Ilgenfritz,<sup>5</sup> A. Yu. Kotov,<sup>2,6</sup> B. Petersson,<sup>7</sup> and S. A. Skinderev<sup>2</sup>

<sup>1</sup>*Institute for High Energy Physics NRC "Kurchatov Institute", Protvino, 142281 Russian Federation*

<sup>2</sup>*Institute of Theoretical and Experimental Physics, 117259 Moscow, Russia*

<sup>3</sup>*Far Eastern Federal University, School of Natural Sciences, 690950 Vladivostok, Russia*

<sup>4</sup>*Moscow Institute of Physics and Technology, Dolgoprudny, 141700 Russia*

<sup>5</sup>*Joint Institute for Nuclear Research, BLTP, 141980 Dubna, Russia*

<sup>6</sup>*National Research Nuclear University MEPhI (Moscow Engineering Physics Institute), Moscow 115409, Russia*

<sup>7</sup>*Humboldt-Universität zu Berlin, Institut für Physik, 12489 Berlin, Germany*

In this paper we report on lattice simulations of  $SU(3)$ -QCD with non-zero chiral chemical potential. We focus on the influence of the chiral chemical potential on the confinement/deconfinement phase transition and the breaking/restoration of chiral symmetry. The simulation is carried out with dynamical Wilson fermions. We find that the critical temperature rises as the chiral chemical potential grows.

## I. INTRODUCTION

The aim of relativistic heavy ion collisions is to study the phase structure of QCD in a more or less unknown region and to explore exotic properties of the phases becoming accessible at high densities of energy and baryonic number. Understanding the interplay of strong electromagnetic fields with the basic mechanisms of QCD has turned out as similarly interesting direction of research since 2008 [1], although not primarily targeted as the high matter density itself, which is characterized by the baryonic chemical potential  $\mu_B$ . This interplay, in particular in the quark-gluon phase, makes its study even more interesting. Here the chiral chemical potential  $\mu_5$  is of central importance.

Indeed, in non-central collisions the strongest magnetic fields on earth ( $qB \sim \mathcal{O}(1..15)m_\pi^2$ ) are created [2] at RHIC and LHC with a lifetime of few fm/c in each collision. There exist also electric field fluctuations of a similar order of magnitude [3]. If electric and magnetic fields are coupled through the Ohmic and anomalous conductivities of the plasma, the magnetic field due to the spectators is practically unaltered [4].

The coupling between color and electromagnetic fields belongs to field of phenomena possible due to the axial anomaly [5–7]. Besides the well-known role it is playing in the QCD vacuum at  $T = 0$ , it has a constitutive role under the extremal conditions which exist in the intermediate non-hadronic phase as well as in certain condensed matter systems [8] as recently has been noticed.

The violation of  $U_A(1)$  symmetry (which is not spontaneously broken but rather due to the topological vacuum structure at  $T = 0$ ) is well-known in the form of mass splittings between hadrons [9, 10] (and signalled by further observables like  $\Delta = \langle \pi\pi \rangle - \langle \delta\delta \rangle$ , the splitting between the  $\pi$  and  $\delta$  norms, the  $T$  dependence of the Dirac spectral density, and of the topological susceptibility  $\chi_{\text{top}}$ ). The  $U_A(1)$  symmetry will be restored in the temperature range up to few times  $T_c$ . How this happens in detail in real QCD in contrast to pure Yang-Mills theory [11], is under intensive study on the lattice [12–17].

Instead of topological charge appearing (at the infrared scale) in the form of Euclidean instantons or dyons [18]), the axial anomaly will play a dynamical role during the short time of existence of liberated quarks. Mesoscopic domains of (almost classical) strongly CP violating gluon fields are created during the initial stadium of a collision (with color electric and magnetic fields  $\vec{E}^a || \vec{B}^a || \text{collision axis}$ ). This is believed to lead to the accumulation of a chiral imbalance between quarks,  $n_5 = n(\text{lefthanded}) - n(\text{righthanded}) \neq 0$  (with random sign and strength). The analogon of instanton tunneling at high temperature, the sphaleron transitions over-the-barrier (frequent at  $T > T_c$ ) give rise to a Chern-Simons diffusion rate  $\Gamma \propto T^4$  which is insufficient to completely wash out the chiral imbalance existing during the lifetime of the high-temperature phase. This, together with the magnetic field  $\vec{B}$  mentioned before, gives rise to anomalous transport of electric current along the magnetic field (the so-called Chiral Magnetic Effect, for a recent report see Ref. [19]), as a remnant of the temporal and local violation of P and CP invariance). Thus, a charge asymmetry w.r.t. the collision plane remains as effect of the electric current  $\vec{J} \propto \mu_5 \vec{H}$  flowing while the deconfined phase has existed. This is the crucial role of  $\mu_5$ . One can also note other phenomena in media with the chiral imbalance [20, 20].

Of course, a precise scenario has to be the result of a space-time transport simulation. In an intermediate step, lattice QCD should explore the multidimensional phase diagram, including (beyond temperature) one or two chemical potentials (baryonic  $\mu_B$  and/or  $\mu_5$ ) and the magnetic field strength. In a first generation of lattice studies, the effect of an external magnetic field on the temperature of the chiral and/or deconfining transition has

been studied [21–23] in isolation. This has led to the discovery of the interplay of opposite tendencies (magnetic catalysis and inverse catalysis of the chiral condensate) at different temperatures. The phase diagram of QCD in a magnetic field has been reviewed in Ref. [24].

Baryonic density  $n_B = (n(\text{quarks}) - n(\text{antiquarks}))/3$ , modelled by  $\mu_B \neq 0$ , still remains difficult to simulate (if not  $\mu_B \ll T$ ) except for  $SU(2)$ . For this model system a simulation with  $N_f = 2$  flavors of staggered fermions has been recently performed [25, 26], following earlier work for  $SU(2)$  (with Wilson fermions) which has been summarized in Ref. [27]. Chiral imbalance, however,  $n_5 = n(\text{lefthanded}) - n(\text{righthanded}) \neq 0$  (expected in the result of the chiral anomaly), can be modelled by a chiral chemical potential  $\mu_5$  without a sign problem. It would be very interesting to study the simultaneous influence of magnetic field and chiral imbalance on the transition temperature. In such studies, as soon as a magnetic field  $\vec{H}$  is included, the induced electric current  $\vec{J} \propto \mu_5 \vec{B}$  would be among the most interesting observables as proposed in Ref. [28].

In a few recent papers [29, 30], our collaboration has begun to study the effect of non-vanishing chiral chemical potential  $\mu_5$  on the transition temperature. We did this first for two-color Yang-Mills theory coupled to staggered fermions without rooting (four flavors). With the present paper we report our results obtained within an extension of our codes to  $SU(3)$  Yang-Mills theory coupled to two flavors of Wilson fermions. Preliminary results have been already reported at “Lattice 2015”.

Section 2 is devoted to the details of the calculation. In section 3 we present our results, and in section 4 we discuss them. In an appendix we study renormalization properties of the chiral condensate with nonzero chiral chemical potential.

## II. DETAILS OF THE SIMULATION.

In the simulation we used the  $SU(3)$  one-plaquette gauge action and a Wilson fermionic action with two degenerate quark flavors. The Dirac operator with non-zero chiral chemical potential has the form [31]

$$D_{xy} = 1 - \kappa \sum_i \left( (1 - \gamma_i) U_i(x) \delta_{x+i,y} + (1 + \gamma_i) U_i^\dagger(y) \delta_{x-i,y} \right) - \kappa \left( (1 - \gamma_4 e^{\mu_5 a \gamma_5}) U_4(x) \delta_{x+4,y} + (1 + \gamma_4 e^{-\mu_5 a \gamma_5}) U_4^\dagger(y) \delta_{x-4,y} \right) \quad (1)$$

Here  $\mu_5$  enters through an additional exponential factor for timelike link variables. In the naive continuum limit  $a \rightarrow 0$ , the fermion action with the Dirac operator (1) corresponds to the fermion action with a chiral chemical potential:

$$S_f^{(cont)} = \int d^4x \bar{\psi} (\partial_\mu \gamma_\mu + ig A_\mu \gamma_\mu + m + \mu_5 \gamma_5 \gamma_0) \psi \quad (2)$$

The Wilson Dirac operator (1) is  $\gamma_5$ -hermitean:

$$\gamma_5 D^\dagger(\mu_5) \gamma_5 = D(\mu_5) \quad (3)$$

This property implies that its determinant  $\det D(\mu_5)$  is real, and in the case of  $N_f = 2$  fermion flavors it is positive. Thus the system has no sign problem and can be simulated by standard Hybrid Monte-Carlo methods.

In our simulations we used Wilson fermions since they allow the introduction of the chiral chemical potential  $\mu_5$  in a local exponential form, what is not possible for staggered fermions. Moreover, calculations with dynamical Wilson fermions require not so many computational resources.

We have performed simulations on a lattice  $4 \times 16^3$ , with  $\kappa = 0.1665$  kept fixed throughout the simulations (performed as  $\beta$ -scan). For  $\beta = 5.32144$  (in the transition region) the chosen  $\kappa$  corresponds to a lattice step size  $a = 0.13$  fm and to a pion mass  $m_\pi = 418$  MeV. Our measured observables are the Polyakov loop, the chiral condensate and their respective susceptibilities. The Polyakov loop and its susceptibility are sensitive to the confinement/deconfinement transition, while the chiral condensate and its susceptibility are sensitive to the chiral symmetry breaking/restoration aspects. We present the observables as functions of  $\beta$  for our scans at four different values of  $\mu_5 a = 0.0, 0.25, 0.5, 0.75$ .

## III. THE RESULTS OF THE SIMULATION

In Figure 1 we show the Polyakov loop and the chiral condensate as functions of  $\beta$  for various  $\mu_5 a$ . The sharp change of observables indicates the position of the phase transition. One clearly sees that nonzero

chiral chemical potential shifts both phase transitions to larger values of  $\beta$ . This means that the transition temperatures increases with  $\mu_5$ . A splitting between both phase transitions is not observed.

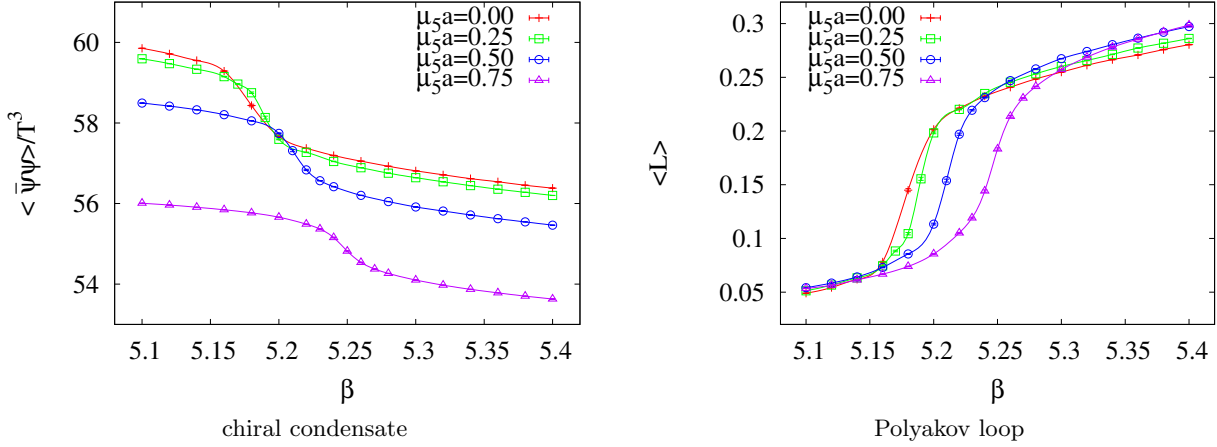


FIG. 1: Chiral condensate and Polyakov loop versus  $\beta$  for four values of  $\mu_5 a$ . The lattice size is  $4 \times 16^3$ , the hopping parameter is  $\kappa = 0.1665$ . Errors are smaller than the data point symbols. The curves are to guide the eye.

In order to confirm our observation and to quantify our results we also have measured the chiral susceptibility and the Polyakov loop susceptibility as functions of  $\beta$ . The results are presented in Figure 2. The peak positions of the susceptibilities correspond to the positions of the respective transition. From these observables one can definitely conclude that the critical temperature grows with increasing  $\mu_5$ .

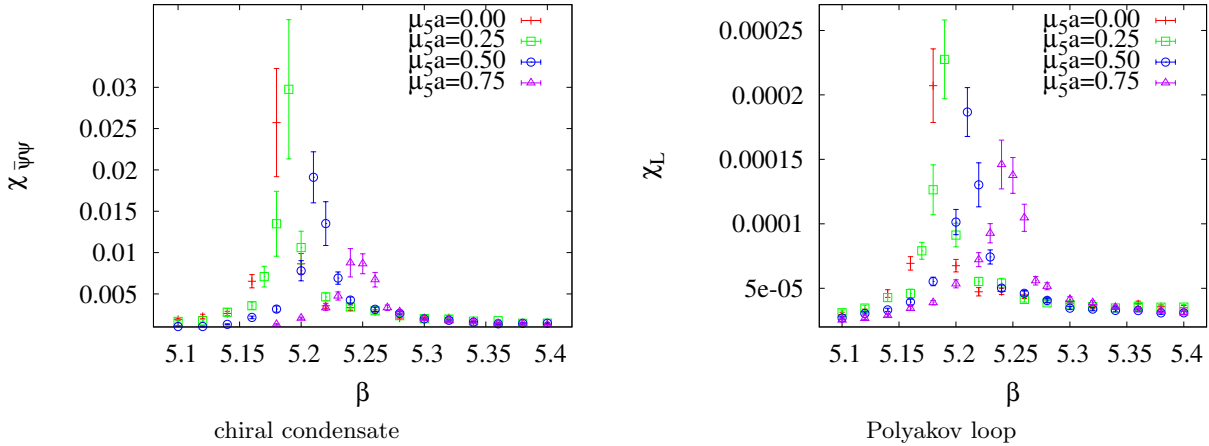


FIG. 2: Chiral susceptibility and Polyakov loop susceptibility versus  $\beta$  for four values of  $\mu_5 a$ . The lattice size is  $4 \times 16^3$ , the hopping parameter is  $\kappa = 0.1665$ .

In order to determine the critical temperatures we fitted the plots for the susceptibilities with a Gaussian function:  $f(\beta) = a_0 + a_1 e^{-(\beta - \beta_c)^2 / \sigma^2}$  (we used 6-7 points near the peak). The dependence of the critical  $\beta_c$  extracted from the fit is shown in Fig. 3. For both susceptibilities it can be described by a quadratic fit:

$$\beta_c = 5.18 + 0.12(\mu_5 a)^2 \quad (4)$$

Using the two-loop  $\beta$ -function, we extract the dependence of the critical temperature on  $\mu_5 a$ . The resulting phase diagram is presented in Fig. 4.

At the end of this section it is important to discuss the ultraviolet divergences of the chiral condensate and of the Polyakov loop and how they affect our results. In the paper [30] it was shown that the introduction of a non-zero chiral chemical potential for staggered fermions leads to an additional logarithmic divergence in

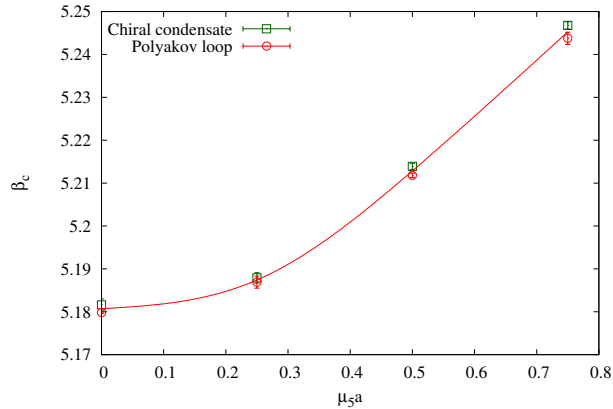


FIG. 3: Critical  $\beta_c$  for the chiral condensate and the Polyakov loop versus  $\mu_5 a$ . The lattice size is  $4 \times 16^3$ , the hopping parameter  $\kappa = 0.1665$ . The curve is to guide the eyes.

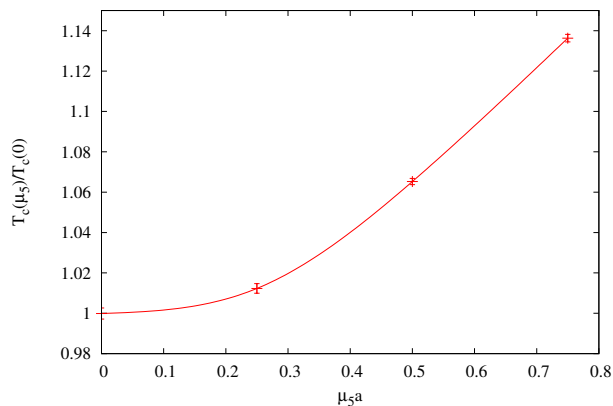


FIG. 4: Critical temperature  $T_c(\mu_5)/T_c(0)$  for the chiral condensate versus  $\mu_5 a$ . The lattice size is  $4 \times 16^3$ , the hopping parameter is  $\kappa = 0.1665$ . The curve is to guide the eyes.

the chiral condensate  $\sim \mu_5^2 \log(a)$ , whereas it does not lead to an additional divergence in the Polyakov loop. In the present work we perform simulations with Wilson fermions, and it is important to study the ultraviolet divergences which appear in the observables in the case of Wilson fermions. First one can repeat all steps in the derivation presented in [30] and show that there are no additional divergences due to  $\mu_5 \neq 0$  for Wilson fermions in the Polyakov loop.

In the Appendix we present an analytical calculation of additional divergences in the chiral condensate for free Wilson fermions. The results of this study allow us to state that there are two additional divergences due to  $\mu_5 \neq 0$ : the first one is logarithmic,  $\sim \mu_5^2 \log(a)$  and the second one is linear  $\sim \mu_5^2/a$ . The logarithmic divergence also exists in the case of staggered fermions [30] with the same coefficient. The linear divergence is new as compared to staggered fermions. We believe that the linear divergence in the chiral condensate appears due to the explicit chiral symmetry breaking of Wilson fermions. Note that the coefficient in front of the linear divergence is negative. So, an increase of the chiral chemical potential leads to a decrease of the chiral condensate. It seems that this behaviour persists in the interacting case. From Fig. 1 one sees that the curves with larger  $\mu_5$  are shifted down compared to the curves with smaller  $\mu_5$ .

Despite the fact that the additional divergences due to  $\mu_5 \neq 0$  give a considerable contribution to the value of the chiral condensate, we believe that there is no influence of the divergences to the position of the breaking/restoration chiral symmetry transition for the following reasons. First, as was noted above there are no divergences in the Polyakov loop. So, if additional divergences had influenced the position of the chiral symmetry breaking/restoration transition, it would be visible as a splitting between the chiral symmetry breaking/restoration and the confinement/deconfinement transitions. But we don't see such splitting. Notice

also that the position of the phase transition manifests itself as a peak of the susceptibility. Evidently, there is no peak due to the additional ultraviolet divergence. All this allows us to state that the conclusions obtained in this paper are not affected by the additional ultraviolet  $\mu_5$  divergence in the chiral condensate.

#### IV. CONCLUSIONS

In this paper we have studied the phase diagram of  $SU(3)$ -QCD with a chiral chemical potential within lattice simulations using  $N_f = 2$  flavors of dynamical Wilson fermions. We have calculated the chiral condensate, the Polyakov loop, the Polyakov loop susceptibility and the chiral susceptibility for different values of the temperature  $T$  and the chiral chemical potential  $\mu_5$  on lattices of size  $4 \times 16^3$ . The main result is that at non-zero values of the chiral chemical potential the critical temperatures of the confinement/deconfinement phase transition and of the chiral-symmetry breaking/restoration phase transition still coincide, and that the common transition is shifted to larger temperatures as  $\mu_5$  increases.

In the present paper we have reported the first investigation of the phase diagram of  $SU(3)$ -QCD with a non-vanishing chiral chemical potential. In the following, one should extrapolate to physical quark masses and to the continuum limit in the hope to confirm the results. This exploration requires much larger computational resources and remains as a task for future studies.

Our result is in agreement with a lattice study of the phase diagram of  $SU(2)$ -QCD [29, 30]. Notice that the simulation described in papers [29, 30] was carried out with staggered fermions which in the continuum corresponds to  $N_f = 4$  flavors. A chiral chemical potential was introduced to the lattice action as an additive term. So, simulations with different fermion discretization and different numbers of colors and flavors give similar results. We believe that this is an argument in favour of the statement that the critical temperature of QCD-like systems rises as the chiral chemical potential is increased.

The studies of the QCD phase diagram with a chiral chemical potential within different effective models have given controversial results. For instance, the authors of papers [32–36] have predicted that the transition shifts to smaller temperatures as  $\mu_5$  increases. At the same time, some of the results obtained in papers [37, 38] imply that the transition shifts to larger temperatures as  $\mu_5$  increases. In paper [38] it was shown that the results of effective models crucially depend on finer details of the models.

In paper [39] the influence of the chiral chemical potential on the chiral symmetry breaking/restoration transition was studied. It was shown that the chiral chemical potential enhances the chiral symmetry breaking and shifts the critical temperature to larger values. The result of our paper confirms this statement.

Besides effective models, the phase diagram of QCD in the  $(\mu_5, T)$ -plane was studied in papers [40, 41] in the framework of Dyson-Schwinger equations. We would like also to mention the paper [42]. In this paper the authors address the question of universality of phase diagrams in QCD and QCD-like theories through the large- $N_c$  equivalence. The authors of these papers found that the critical temperature rises with  $\mu_5$ . These results agree with ours.

#### Acknowledgements

The simulations were performed at the ITEP supercomputer. The work was supported by the Far Eastern Federal University, the Dynasty foundation, by RFBR grants 14-02-01185-a, 15-02-07596-a, 15-32-21117, and by a grant of the FAIR-Russia Research Center.

### Appendix A: Ultraviolet divergences in the chiral condensate

The fermion propagator including the chiral chemical potential for Wilson fermions can be written in the following form

$$S^{\alpha\beta}(x, y) = \frac{\text{elta}^{\alpha\beta}}{L_t L_s^3} \sum_{\{k\}} \sum_{s=\pm 1} e^{ip(x-y)} \frac{m + \frac{\hat{k}^2}{2} - i \sum_{i=1}^3 \gamma_i \sin k_i - i \gamma_4 \sin k_4 \cosh \mu_5 - \cos k_4 \sinh \mu_5 \overline{\gamma}_4 \gamma_5}{\left(m + \frac{\hat{k}^2}{2}\right)^2 + \sin^2 k_4 \cosh^2 \mu_5 + (|\bar{\mathbf{k}}| + s \cos k_4 \sinh \mu_5)^2} \times P(s),$$

$$P(s) = \frac{1}{2} \left( 1 - i s \sum_{i=1}^3 \frac{\gamma_i \sin k_i}{|\bar{\mathbf{k}}|} \overline{\gamma}_4 \gamma_5 \right),$$

$$|\bar{\mathbf{k}}| = \sqrt{\sin^2 k_1 + \sin^2 k_2 + \sin^2 k_3},$$

$$\hat{k}_\mu = 2 \sin(k_\mu/2),$$

$$k_i = \frac{2\pi}{L_s} n_i, i = 1, 2, 3, n_i = 0, \dots, L_s - 1,$$

$$k_4 = \frac{2\pi}{L_t} n_4 + \frac{\pi}{L_t}, n_4 = 0, \dots, L_t - 1.$$

Here  $m$  and  $\mu_5$  are mass and chiral chemical potential in lattice units,  $\alpha, \beta$  are color indices, the sum is taken over all possible values of  $(n_1, n_2, n_3, n_4)$  (lattice coordinates).

In the limit  $L_s, L_t \rightarrow \infty$  the condensate can be written as

$$\langle \bar{\psi} \psi \rangle = Tr[S(x, x)] = 6 \int_{-\pi}^{\pi} \frac{d^4 k}{(2\pi)^4} \sum_{s=\pm 1} \frac{m + \frac{\hat{k}^2}{2}}{\left(m + \frac{\hat{k}^2}{2}\right)^2 + \sin^2 k_4 \cosh^2 \mu_5 + (|\bar{\mathbf{k}}| + s \cos k_4 \sinh \mu_5)^2}; \quad (\text{A1})$$

To calculate the integral in formula (A1) we use the algebraic method, explained in [43, 44]. The Taylor expansion in  $\mu_5$  tends to

$$\frac{1}{6} \langle \bar{\psi} \psi \rangle = 2 \int_{-\pi}^{\pi} \frac{d^4 k}{(2\pi)^4} \frac{m + \frac{\hat{k}^2}{2}}{\left(m + \frac{\hat{k}^2}{2}\right)^2 + \sum_{\mu} \bar{k}_{\mu}^2} + \mu_5^2 \left( -\frac{2(m + \frac{\hat{k}^2}{2})}{\left(\left(m + \frac{\hat{k}^2}{2}\right)^2 + \sum_{\mu} \bar{k}_{\mu}^2\right)^2} + \frac{8 \cos^2 k_4 |\bar{\mathbf{k}}|^2 (m + \frac{\hat{k}^2}{2})}{\left(\left(m + \frac{\hat{k}^2}{2}\right)^2 + \sum_{\mu} \bar{k}_{\mu}^2\right)^3} \right) + O(\mu_5^4).$$

The first term in this expression is just the loop integral for  $\langle \bar{\psi} \psi \rangle$  without chiral chemical potential. The expression for this integral in the limit  $a \rightarrow 0$  can be written as follows

$$2 \int_{-\pi}^{\pi} \frac{d^4 k}{(2\pi)^4} \frac{m + \frac{\hat{k}^2}{2}}{\left(m + \frac{\hat{k}^2}{2}\right)^2 + \sum_{\mu} \bar{k}_{\mu}^2} = c_0 + c_1 m + c_2 m^2 + m^3 \left( \frac{\log m^2}{8\pi^2} + c_3 \right) + O(m^4) \quad (\text{A2})$$

$$c_0 = 0.469363, \quad c_1 = -0.067967, \quad c_2 = -0.023613, \quad c_3 = -0.075829.$$

The second term in (A2) we can calculate similarly. The result of the calculation can be written as follows

$$\int_{-\pi}^{\pi} \frac{d^4 k}{(2\pi)^4} \left( -\frac{2(m + \frac{\hat{k}^2}{2})}{\left(\left(m + \frac{\hat{k}^2}{2}\right)^2 + \sum_{\mu} \bar{k}_{\mu}^2\right)^2} + \frac{8 \cos^2 k_4 |\bar{\mathbf{k}}|^2 (m + \frac{\hat{k}^2}{2})}{\left(\left(m + \frac{\hat{k}^2}{2}\right)^2 + \sum_{\mu} \bar{k}_{\mu}^2\right)^3} \right) = c_4 + m \left( -\frac{\log m^2}{4\pi^2} + c_5 \right) + O(m^2) \quad (\text{A3})$$

$$c_4 = -0.010738, \quad c_5 = 0.045999.$$

We have checked the two last formulas numerically. Restoring the lattice spacing  $a$  in our results we get

$$\langle \bar{\psi} \psi \rangle = \frac{6c_0}{a^3} + \frac{6c_1 m}{a^2} + \frac{6c_2 m^2}{a} + m^3 \left( \frac{3 \log(ma)}{2\pi^2} + 6c_3 \right) + \frac{6c_4 \mu_5^2}{a} + \mu_5^2 m \left( -\frac{3 \log(ma)}{\pi^2} + 6c_5 \right). \quad (\text{A4})$$

The first line in formula (A4) represents the chiral condensate without chiral chemical potential, whereas the second line is the contribution due to non-zero  $\mu_5$ . It is seen that there is an additional logarithmic divergence due to  $\mu_5 \neq 0$ . The same divergence with the same coefficient appears in the case of staggered fermions [30]. However, there is also a linear divergence  $\sim \mu_5^2/a$  which is absent in the case of staggered fermions. We believe

that this linear divergence in the chiral condensate appears due to the explicit chiral symmetry breaking of Wilson fermions. Note that the coefficient in front of the linear divergence is negative. So, an increase of the chiral chemical potential leads to a decrease of the chiral condensate what is seen in Fig.1.

- 
- [1] Dmitri E. Kharzeev, Larry D. McLerran, and Harmen J. Warringa. The Effects of topological charge change in heavy ion collisions: 'Event by event P and CP violation'. *Nucl. Phys.*, A803:227–253, 2008.
- [2] V. Skokov, A. Yu. Illarionov, and V. Toneev. Estimate of the magnetic field strength in heavy-ion collisions. *Int. J. Mod. Phys.*, A24:5925–5932, 2009.
- [3] Adam Bzdak and Vladimir Skokov. Event-by-event fluctuations of magnetic and electric fields in heavy ion collisions. *Phys. Lett.*, B710:171–174, 2012.
- [4] L. McLerran and V. Skokov. Comments About the Electromagnetic Field in Heavy-Ion Collisions. *Nucl. Phys.*, A929:184–190, 2014.
- [5] Stephen L. Adler. Axial vector vertex in spinor electrodynamics. *Phys. Rev.*, 177:2426–2438, 1969.
- [6] J. S. Bell and R. Jackiw. A PCAC puzzle:  $\pi^0 \rightarrow \gamma\gamma$  in the sigma model. *Nuovo Cim.*, A60:47–61, 1969.
- [7] William A. Bardeen. Anomalous Currents in Gauge Field Theories. *Nucl. Phys.*, B75:246, 1974.
- [8] Dmitri E. Kharzeev. Topology, magnetic field, and strongly interacting matter. *Ann. Rev. Nucl. Part. Sci.*, 65:193–214, 2015.
- [9] Edward Witten. Current Algebra Theorems for the U(1) Goldstone Boson. *Nucl. Phys.*, B156:269, 1979.
- [10] G. Veneziano. U(1) Without Instantons. *Nucl. Phys.*, B159:213–224, 1979.
- [11] V. G. Bornyakov, E. M. Ilgenfritz, B. V. Martemyanov, V. K. Mitrjushkin, and M. Mller-Preussker. Topology across the finite temperature transition studied by overimproved cooling in gluodynamics and QCD. *Phys. Rev.*, D87(11):114508, 2013.
- [12] Michael I. Buchoff et al. QCD chiral transition, U(1)A symmetry and the dirac spectrum using domain wall fermions. *Phys. Rev.*, D89(5):054514, 2014.
- [13] Sayantan Sharma, Viktor Dick, Frithjof Karsch, Edwin Laermann, and Swagato Mukherjee. Investigation of the  $U_A(1)$  in high temperature QCD on the lattice. *PoS, LATTICE2013:164*, 2014.
- [14] Sinya Aoki, Hidenori Fukaya, and Yusuke Taniguchi. Chiral symmetry restoration, eigenvalue density of Dirac operator and axial U(1) anomaly at finite temperature. *Phys. Rev.*, D86:114512, 2012.
- [15] Guido Cossu, Sinya Aoki, Hidenori Fukaya, Shoji Hashimoto, Takashi Kaneko, Hideo Matsufuru, and Jun-Ichi Noaki. Finite temperature study of the axial U(1) symmetry on the lattice with overlap fermion formulation. *Phys. Rev.*, D87(11):114514, 2013. [Erratum: *Phys. Rev.* D88,no.1,019901(2013)].
- [16] Bastian B. Brandt, Anthony Francis, Harvey B. Meyer, Hartmut Wittig, and Owe Philipsen. QCD thermodynamics with two flavours of Wilson fermions on large lattices. *PoS, LATTICE2012:073*, 2012.
- [17] Bastian B. Brandt, Anthony Francis, Harvey B. Meyer, Owe Philipsen, and Hartmut Wittig. QCD thermodynamics with O(a) improved Wilson fermions at  $N_f = 2$ . *PoS, LATTICE2013:162*, 2014.
- [18] E. M. Ilgenfritz, B. V. Martemyanov, and M. Muller-Preussker. Topology near the transition temperature in lattice gluodynamics analyzed by low lying modes of the overlap Dirac operator. *Phys. Rev.*, D89(5):054503, 2014.
- [19] D. E. Kharzeev, J. Liao, S. A. Voloshin, and G. Wang. Chiral Magnetic Effect in High-Energy Nuclear Collisions — A Status Report. 2015.
- [20] Andrey V. Sadofyev and Yi Yin. The charmonium dissociation in an "anomalous wind". 2015.
- [21] Massimo D'Elia, Swagato Mukherjee, and Francesco Sanfilippo. QCD Phase Transition in a Strong Magnetic Background. *Phys. Rev.*, D82:051501, 2010.
- [22] G. S. Bali, F. Bruckmann, G. Endrodi, Z. Fodor, S. D. Katz, S. Krieg, A. Schafer, and K. K. Szabo. The QCD phase diagram for external magnetic fields. *JHEP*, 02:044, 2012.
- [23] E. M. Ilgenfritz, M. Kalinowski, M. Muller-Preussker, B. Petersson, and A. Schreiber. Two-color QCD with staggered fermions at finite temperature under the influence of a magnetic field. *Phys. Rev.*, D85:114504, 2012.
- [24] Jens O. Andersen, William R. Naylor, and Anders Tranberg. Phase diagram of QCD in a magnetic field: A review. 2014.
- [25] V. V. Braguta, A. Yu. Kotov, A. A. Nikolaev, and S. N. Valgushev. Lattice simulation of  $QC_2D$  with  $N_f = 2$  at non-zero baryon density. In *Proceedings, 33rd International Symposium on Lattice Field Theory (Lattice 2015)*, 2015.
- [26] V. V. Braguta, A. Yu. Kotov, A. A. Nikolaev, and S. N. Valgushev. Lattice simulation study of SU(2) QCD with a nonzero baryon density. *JETP Lett.*, 101(11):732–734, 2015. [Pisma Zh. Eksp. Teor. Fiz.101,no.11,827829(2015)].
- [27] Seamus Cotter, Pietro Giudice, Simon Hands, and Jon-Ivar Skullerud. Towards the phase diagram of dense two-color matter. *Phys. Rev.*, D87(3):034507, 2013.
- [28] Arata Yamamoto. Chiral Magnetic Effect on the Lattice. *Lect. Notes Phys.*, 871:387–397, 2013.
- [29] V. V. Braguta, V. A. Goi, M. Ilgenfritz, A. Yu. Kotov, A. V. Molochkov, and M. Mller-Preussker. Study of the phase diagram of SU(2) quantum chromodynamics with nonzero chirality. *JETP Lett.*, 100(9):547–549, 2015. [Pisma Zh. Eksp. Teor. Fiz.100,no.9,623(2015)].

- [30] V. V. Braguta, V. A. Goy, E. M. Ilgenfritz, A. Yu. Kotov, A. V. Molochkov, M. Muller-Preussker, and B. Petersson. Two-Color QCD with Non-zero Chiral Chemical Potential. *JHEP*, 06:094, 2015.
- [31] Arata Yamamoto. Chiral magnetic effect in lattice QCD with a chiral chemical potential. *Phys. Rev. Lett.*, 107:031601, 2011.
- [32] Kenji Fukushima, Marco Ruggieri, and Raoul Gatto. Chiral magnetic effect in the PNJL model. *Phys. Rev.*, D81:114031, 2010.
- [33] M. N. Chernodub and A. S. Nedelin. Phase diagram of chirally imbalanced QCD matter. *Phys. Rev.*, D83:105008, 2011.
- [34] Raoul Gatto and Marco Ruggieri. Hot Quark Matter with an Axial Chemical Potential. *Phys. Rev.*, D85:054013, 2012.
- [35] Jingyi Chao, Pengcheng Chu, and Mei Huang. Inverse magnetic catalysis induced by sphalerons. *Phys. Rev.*, D88:054009, 2013.
- [36] Lang Yu, Hao Liu, and Mei Huang. Spontaneous generation of local CP violation and inverse magnetic catalysis. *Phys. Rev.*, D90(7):074009, 2014.
- [37] Alexander A. Andrianov, Domenec Espriu, and Xumeu Planells. Chemical potentials and parity breaking: the Nambu-Jona-Lasinio model. *Eur. Phys. J.*, C74(2):2776, 2014.
- [38] Lang Yu, Hao Liu, and Mei Huang. The effect of the chiral chemical potential on the chiral phase transition in the NJL model with different regularization schemes. 2015.
- [39] V. V. Braguta and A. Yu. Kotov. To be published.
- [40] Bin Wang, Yong-Long Wang, Zhu-Fang Cui, and Hong-Shi Zong. Effect of the chiral chemical potential on the position of the critical endpoint. *Phys. Rev.*, D91(3):034017, 2015.
- [41] Shu-Sheng Xu, Zhu-Fang Cui, Bin Wang, Yuan-Mei Shi, You-Chang Yang, and Hong-Shi Zong. Chiral phase transition with a chiral chemical potential in the framework of Dyson-Schwinger equations. *Phys. Rev.*, D91(5):056003, 2015.
- [42] Masanori Hanada and Naoki Yamamoto. Universality of phase diagrams in QCD and QCD-like theories. *PoS, LATTICE2011:221*, 2011.
- [43] Giuseppe Burgio, Sergio Caracciolo, and Andrea Pelissetto. Algebraic algorithm for the computation of one loop Feynman diagrams in lattice QCD with Wilson fermions. *Nucl. Phys.*, B478:687–722, 1996.
- [44] Stefano Capitani. Lattice perturbation theory. *Phys. Rept.*, 382:113–302, 2003.